

The JAK-Inhibitor Tofacitinib Rescues Human Intestinal Epithelial Cells and Colonoids from Cytokine-Induced Barrier Dysfunction

Anica Sayoc-Becerra,* Moorthy Krishnan, PhD,* Shujun Fan, PhD,[†] Jossue Jimenez,* Rebecca Hernandez,* Kyle Gibson,* Reyna Preciado,* Grant Butt, PhD,[†] and Declan F. McCole, PhD*

Background: Alterations to epithelial tight junctions can compromise the ability of the epithelium to act as a barrier between luminal contents and the underlying tissues, thereby increasing intestinal permeability, an early critical event in inflammatory bowel disease (IBD). Tofacitinib (Xeljanz), an orally administered pan-Janus kinase (JAK) inhibitor, was recently approved for the treatment of moderate to severe ulcerative colitis. Nevertheless, the effects of tofacitinib on intestinal epithelial cell functions are largely unknown. The aim of this study was to determine if JAK inhibition by tofacitinib can rescue cytokine-induced barrier dysfunction in intestinal epithelial cells (IECs).

Methods: T₈₄ IECs were used to evaluate the effects of tofacitinib on JAK-signal transducer and activator of transcription (STAT) activation, barrier permeability, and expression and localization of tight junction proteins. The impact of tofacitinib on claudin-2 promoter activity was assessed in HT-29 IECs. Tofacitinib rescue of barrier function was also tested in human colonic stem cell-derived organoids.

Results: Pretreatment with tofacitinib prevented IFN- γ -induced decreases in transepithelial electrical resistance (TER) and increases in 4 kDa FITC-dextran permeability (FD4), partly due to claudin-2 transcriptional regulation and restriction of ZO-1 rearrangement at tight junctions. Although tofacitinib administered after IFN- γ challenge only partially normalized TER and claudin-2 levels, FD4 permeability and ZO-1 localization were fully recovered. The IFN- γ -induced FD4 permeability in primary human colonoids was fully rescued by tofacitinib.

Conclusions: These data suggest differential therapeutic efficacy of tofacitinib in the rescue of pore vs leak-tight junction barrier defects and indicate a potential contribution of improved epithelial barrier function to the beneficial effects of tofacitinib in IBD patients.

Key Words: claudin-2, organoids, IFN- γ , intestinal permeability, STAT1, ZO-1

INTRODUCTION

Inflammatory bowel disease (IBD) comprises the chronic inflammatory conditions Crohn's disease (CD) and ulcerative colitis (UC), in which the immune system mounts an abnormal response to normal constituents in the gastrointestinal tract in events driven by both genetic and environmental risk factors. Damage to the intestinal epithelium or disruption of the apical tight junctions can compromise the ability of the epithelium to serve as a barrier between luminal contents and the underlying

tissues.¹⁻⁴ Tight junctions (TJs) connect neighboring intestinal epithelial cells (IECs), in concert with adherens junctions, and act as a selective barrier to paracellular solute permeability.²⁻⁴ Reconfiguration of tight junctions through removal or insertion of specific proteins can increase intestinal permeability.^{1-2, 5} This facilitates dysregulated fluid and electrolyte transport, which can contribute to one of the main clinical symptoms of IBD: diarrhea.^{1, 2, 5} Changes in expression or localization of tight junction proteins can also increase access of bacterial products into the lamina propria, which can trigger inappropriate immune responses and contribute to the pathogenesis of IBD.^{2, 5} Permeability is an important parameter of intestinal homeostasis as increases in intestinal permeability have been shown to precede colonic inflammation in humans and animal models of colitis.⁶⁻⁸

Paracellular permeability can feature both charge- and size-selective dependent or independent events, and these functional characteristics of "pore" and "leak" barrier defects, respectively, are regulated in general by different assemblies of tight junction proteins and associated signaling pathways.⁹ The claudin family of transmembrane proteins is a major structural component of the tight junction that is both size- and charge-selective for the passive paracellular movement of fluid and solutes.^{3, 4, 10} One prominent member of this family is claudin-2, which forms cation-selective pores, thus making the epithelial barrier more permissive to paracellular flux of

Received for publications May 2, 2019; Editorial Decision September 12, 2019.

From the *Division of Biomedical Sciences, School of Medicine, University of California, Riverside, CA, USA; [†]Department of Physiology, School of Biomedical Sciences, University of Otago, Dunedin, New Zealand

Supported by: NIH-2R01-DK091281 (DFM); ASPIRE-Pfizer JAK-STAT in IBD Research Awards, 2016 (W1214999), 2017 (W1227049) (DFM).

Conflicts of interest: DFM has received investigator-initiated research awards from the makers of tofacitinib (Pfizer Inc.) through the ASPIRE-Pfizer JAK-STAT in IBD Research Program.

Address correspondence to: Declan F. McCole, PhD, Division of Biomedical Sciences, School of Medicine, University of California–Riverside, 307 School of Medicine Research Building, 900 University Avenue, Riverside, CA, 92521 USA. E-mail: declan.mccole@ucr.edu.

© 2019 Crohn's & Colitis Foundation. Published by Oxford University Press. All rights reserved. For permissions, please e-mail: journals.permissions@oup.com.

doi: 10.1093/ibd/izz266

Published online 21 November 2019

fluid and cations, predominantly Na^+ , which can decrease the electrical resistance across the epithelium.^{11,12} This TJ protein is clinically relevant because claudin-2 expression is increased in IBD and is regarded as a biomarker of increased paracellular permeability to electrolyte flux.^{1,13,14} Claudin-2 is upregulated by several pro-inflammatory cytokines, including interferon-gamma ($\text{IFN-}\gamma$), and its induction is partly dependent on STAT1 binding to the claudin-2 promoter to regulate transcriptional expression.¹⁵ Apart from claudins, which predominantly regulate ion and water flux, transmembrane proteins occludin and tricellulin help control paracellular passage of larger, uncharged solutes.¹⁶⁻¹⁸ In addition to transmembrane proteins, peripheral membrane proteins, such as zonula occludens 1 (ZO-1), play crucial roles in both the assembly and regulation of tight junctions.¹⁹ This is accomplished, at least in part, by their multiple domains that allow them to act as scaffolding proteins through interactions with other integral or regulatory proteins, including various claudins, occludin, and actin.²⁰⁻²² Further increasing the versatility of these structures is that the proteins composing this complex conglomeration are highly dynamic. Thus, a typical feature of barrier dysfunction is altered membrane localization or increased internalization of tight junction proteins in the presence or absence of changes in overall expression.²³⁻²⁵ Therefore, appropriate localization of tight junction-associated proteins, such as ZO-1, is an essential factor in the maintenance of the epithelial barrier.

There are currently >203 candidate genes associated with the risk of onset of IBD, most of which are involved in regulating the immune system's interaction with IECs and microbial flora.²⁶⁻²⁸ A number of these genes are involved in regulating the Janus kinase-signal transduction and transcription (Janus kinase-signal transducer and activator of transcription [JAK-STAT]) pathway, which can be activated by several cytokines involved in IBD, including $\text{IFN-}\gamma$, whose expression by CD4^+ T lymphocytes is increased in inflamed intestinal tissues from CD patients compared with control subjects.^{26,29} The effects of $\text{IFN-}\gamma$ are mediated through the JAK-STAT signaling pathway, with specificity for activation of JAK1 and JAK2.³⁰ Phosphorylated levels of their downstream targets STAT1 and STAT3 are elevated in CD patients compared with controls.³¹ In addition, $\text{IFN-}\gamma$ reduces epithelial barrier function by decreasing electrical resistance across intestinal cell monolayers and increasing permeability to macromolecules in vitro.³²⁻³⁷

Inhibitors of JAK-STAT signaling have emerged as a new therapeutic focus in IBD. Tofacitinib (Xeljanz, CP-690550), an orally administered pan-JAK inhibitor was originally approved for the treatment of rheumatoid arthritis.³⁸ Tofacitinib is now FDA-approved for the treatment of moderate to severe UC and has been studied in phase 2 clinical trials in CD.³⁹⁻⁴¹ Tofacitinib is a reversible, competitive small molecule inhibitor that binds to the adenosine triphosphate (ATP) binding site in the catalytic cleft of the kinase domain of JAKs. Tofacitinib structurally mimics ATP without the triphosphate group. Thus by binding to the

ATP site, it inhibits the phosphorylation and activation of JAK, thereby preventing the phosphorylation and activation of downstream STAT proteins. Tofacitinib functions intracellularly and possesses high in vitro passive permeability consistent with intracellular entry by transcellular diffusion.³⁸ Although studies on JAK-STAT signaling therapeutics have focused on immune cell targets and clinical primary endpoints, it is poorly understood how these agents affect IEC functions, such as the increase in intestinal permeability associated with IBD. In this study, we investigated whether tofacitinib exerts a direct beneficial effect on IEC barrier function and if it can rescue tight junction modifications caused by an IBD-relevant inflammatory cytokine, $\text{IFN-}\gamma$.

MATERIALS AND METHODS

Materials

Human recombinant $\text{IFN-}\gamma$ (Roche, Mannheim, Germany), tofacitinib (MedChemExpress, Monmouth Junction, NJ; Selleckchem, Houston, TX), and dimethyl sulfoxide (DMSO; Sigma-Aldrich, St. Louis, MO) were obtained from the sources indicated. $\text{IFN-}\gamma$ was used at a concentration of 1000 U/mL, equivalent to 50 ng/mL, unless otherwise stated.

Cells

Human T_{84} and HT-29 IECs were grown in Dulbecco's modified Eagle's Medium/Ham's F-12 (DMEM/F12) 50:50 Mix (Corning, Tewksbury, MA) and McCoy's 5A medium (Corning, Tewksbury, MA), respectively, and supplemented with 10% heat-inactivated fetal bovine serum (FBS; Gibco, Waltham, MA), 1% L-glutamine (Invitrogen, Carlsbad, CA), and 1% penicillin (100 U/mL)/streptomycin (100 $\mu\text{g/mL}$) (Corning, Tewksbury, MA). Cells were cultured on standard cell culture plates or transwell membranes (0.4- μm pore size, 1.12- cm^2 surface area, Corning, Tewksbury, MA) in a 37°C incubator maintained at 5% CO_2 /air mix. IECs were serum-deprived overnight before treatments with tofacitinib, DMSO, and/or $\text{IFN-}\gamma$. For cells grown on transwells, tofacitinib and DMSO were administered to the apical compartment, and $\text{IFN-}\gamma$ was added to the basolateral compartment. $\text{IFN-}\gamma$ was administered at a concentration (1000 U/mL; 24 hrs) previously shown to decrease TER without causing damage to the epithelial monolayer.¹⁵

Determination of Epithelial Monolayer Resistance and Paracellular Permeability

Transepithelial electrical resistance (TER) of T_{84} monolayers grown on transwells was measured using the EVOM2 Epithelial Voltohmmeter (World Precision Instruments, Sarasota, FL) and chopstick electrode set for EVOM2 (World Precision Instruments, Sarasota, FL). The average of 3 measurements per transwell was calculated and expressed in $\text{Ohms}\cdot\text{cm}^2$.

Macromolecular paracellular permeability was measured as the flux of 4-kilodalton fluorescein isothiocyanate-dextran (4 kDa FITC-dextran; FD4, Sigma-Aldrich, St. Louis, MO) across polarized T₈₄ monolayers. After TER measurements, cells were washed twice with and equilibrated in phosphate buffered saline (PBS) with CaCl₂ and MgCl₂ for 30 minutes at 37°C. Then FD4 at a final concentration of 1 mg/mL was added to the apical compartment of the monolayers. After 2 hours of incubation at 37°C, 50 µL of the basolateral solution was sampled in duplicate and fluorescence was detected using a microplate reader (Promega, Madison, WI). Based on relative fluorescence units (RFU), FD4 concentrations were calculated against a standard curve and expressed as percent change from untreated cells.

Preparation of Whole Cell Protein Lysates

At the end of the experimental period, cells were washed twice with ice-cold PBS. Ice-cold radioimmunoprecipitation assay lysis buffer (50 mM Tris-chloride pH 7.4, 150 mM sodium chloride, 1% NP-40, 0.5% sodium deoxycholate, 0.1% sodium dodecyl sulfate [SDS]) supplemented with protease (Roche, Mannheim, Germany) and phosphatase inhibitors (sodium orthovanadate, Phosphatase Inhibitor Cocktail 2 and 3, Sigma-Aldrich, St. Louis, MO) was added, and cells were incubated at 4°C for 15 minutes. Cells were scraped into microcentrifuge tubes and sonicated on ice at 30% amplitude, 10-second on/off intervals for 20 seconds using the Q125 Sonicator (QSonica Sonicators, Newtown, CT). Cell lysates were centrifuged at 16,200 × g for 10 minutes to remove insoluble material, and supernatants were collected into new microcentrifuge tubes. An aliquot of each sample was used to determine protein concentration using Pierce Bicinchoninic Acid Protein Assay Kit reagents (ThermoFisher Scientific, Waltham, MA). Protein content was adjusted with lysis buffer to ensure the same amount of total protein in each sample, and then mixed with loading buffer (60 mM Tris-Cl pH 6.8, 2% SDS, 5% β-mercaptoethanol, 0.01% bromophenol blue, 10% glycerol). All samples were boiled at 95°C for 10 minutes and loaded on SDS-polyacrylamide gels for Western blotting.

Western Blot Analysis

Whole cell proteins were resolved on 7% or 11% SDS-polyacrylamide gels at 100 V at room temperature and then transferred onto polyvinylidene difluoride membranes (EMD Millipore, Darmstadt, Germany) for 2 hours at 250 mA in 4°C. Membranes were blocked with 5% nonfat milk in Tris-buffered saline with 0.1% Tween-20 (TBS-T) for 1 hour at room temperature, followed by further incubation with claudin-2 (1:1000, #32-5600, Invitrogen, Camarillo, CA), claudin-1 (1:1000, #51-9000, Thermo Fisher Scientific, Rockford, IL), claudin-4 (1:1000, #32-9400, Invitrogen, Camarillo, CA), claudin-15 (1:1000, #32-9800, Invitrogen, Frederick, MD), ZO-1 (1:1000, #61-7300, Thermo Fisher Scientific, Waltham, MA), occludin

(1:1000, #71-1500 for T₈₄ cells, Invitrogen, Carlsbad, CA; #40-4700 for the colonoids, Rockford, IL), tricellulin/marvel D2 (1:1000, ab203567, Abcam, Cambridge, MA), phospho-JAK1 (1:1000, #3331, Cell Signaling Technology, Danvers, MA), JAK1 (1:1000, #3344, Cell Signaling Technology, Danvers, MA), phospho-STAT1 (1:500, #9167, Cell Signaling Technology, Danvers, MA), STAT1 (1:1000, #9175, Cell Signaling Technology, Danvers, MA), phospho-STAT3 (1:1000, #9145, Cell Signaling Technology, Danvers, MA), STAT3 (1:1000, #9139, Cell Signaling Technology, Danvers, MA) and β-actin (1:8000, #A5316, Sigma-Aldrich, St. Louis, MO) primary antibodies overnight at 4°C. The following day, membranes were subjected to 5-minute washes (x5) with TBS-T and then incubated with peroxidase-conjugated secondary antibodies (goat antimouse [#115-036-062] or goat antirabbit [#111-036-045], Jackson Immunoresearch Laboratories, Inc. West Grove, PA) diluted at 1:5000 in 1% nonfat milk in TBS-T for 1 hour at room temperature. This was followed by 5-minute washes (x5) with TBS-T. Membranes were then incubated with SuperSignal West Pico PLUS Chemiluminescent Substrate solution (ThermoFisher Scientific, Waltham, MA) according to manufacturer's directions and exposed to film (LabScientific Inc., Highlands, NJ). Densitometric analysis of the blots was performed using ImageJ software (National Institutes of Health, Bethesda, MD).⁴²

Claudin-2 Promoter Luciferase Reporter Assay

Claudin-2 promoter activity assay was performed in HT-29 IECs as previously described.¹⁵ Briefly, a gene construct spanning the -900 bp to +112 bp region of the human *CLDN2* gene promoter (Integrated DNA Technologies, Coralville, IA) was cloned into the pGL3-Basic Luciferase Reporter Vector (Promega, Madison, WI) using the restriction enzymes NheI and KpnI. The sequence of the product was confirmed using sequencing analyses.

The HT-29 cells were grown in 12-well cell culture plates until ~60% confluence was reached. The following day, cells were cotransfected with the *CLDN2* promoter-luciferase reporter construct and a reference construct containing *Renilla reniformis* luciferase (pRL) and the HSV-thymidine kinase (TK) promoter (Promega, Madison, WI) using Effectene Transfection Reagent kit (Qiagen, Hilden, Germany) per manufacturer's instructions. Twenty-four hours later, cells were pretreated with tofacitinib or DMSO for 1 hour followed by IFN-γ for 24 hours. Luciferase activities were measured using the Dual-Luciferase Reporter Assay System (Promega, Madison, WI) and a Glomax Multidetection System (Promega, Madison, WI). Firefly luciferase activity was normalized to *Renilla* luciferase activity.

ZO-1 and Occludin Immunofluorescence

After experimental treatments, T₈₄ IECs grown on glass coverslips were washed twice with PBS, fixed with ice-cold

methanol for 10 minutes at -20°C , and then washed 3 times with PBS. Fixed cells were permeabilized with 0.5% Triton X-100 in PBS for 30 minutes at room temperature and then washed again with PBS 3 times. After blocking with 10% normal donkey serum (NDS, Jackson Immunoresearch Laboratories, Inc. West Grove, PA) diluted in 0.04% PBS-Tween 20 (PBS-T) for 1 hour at room temperature, cells were stained with ZO-1 (#61-7300, ThermoFisher Scientific, Waltham, MA) or occludin (#71-1500, Invitrogen, Carlsbad, CA) primary antibody diluted at 1:200 in 1% NDS in PBS-T overnight at 4°C . Fixed cells were then washed 5 times with PBS-T followed by incubation with Alexa 488-conjugated donkey antirabbit secondary antibody (#711-545-152, Jackson Immunoresearch Laboratories, Inc., West Grove, PA) diluted at 1:200 in 1% PBS-T for 1 hour at room temperature. Stained cells were washed 5 times with PBS-T and once with PBS and then mounted in ProLong Gold Antifade Mountant with DAPI (Invitrogen, Carlsbad, CA) before visualization.

Images for ZO-1 immunofluorescence were captured using a Leica DM5500 microscope attached with a DFC365 FX camera using a 63x oil immersion objective with an additional 2x digital zoom. Individual images were converted into .tiff files with the LAS-AF Lite software, and Adobe Photoshop was used to create the final figures. The number of intercellular gaps per treatment was determined in 8 images per coverslip covering 4 different fields of view.

Z-stack images of occludin immunofluorescence were obtained using a CSU-X-1 spinning-disk confocal imager (Yokogawa, Japan) attached to a Zeiss Axio Observer inverted microscope (Carl Zeiss, Thornwood, NY). Original magnification of 63x was used. Micro-Manager Imaging Software (Molecular Devices, Sunnyvale, CA) was used to control the hardware (confocal microscope and the Prim 95B digital camera). Avi movie files were generated from z-stack images using ImageJ.⁴²

Human Colonoid Cultures

Epithelial-derived colonic organoids (colonoids) were grown from crypts isolated from biopsy samples obtained from transverse colon of patients undergoing elective colonoscopy, primarily for colon cancer screening. Written informed consent was obtained before specimen collection, and studies were approved by the Health and Disabilities Ethics Committee (New Zealand, Ethics No. 13/STH/155). The following protocols for colonoid isolation and culture were adapted from methods established in Sato, et al.⁴³ The biopsy samples were collected in ice-cold DMEM/F12 medium containing antibiotics (1% penicillin/streptomycin, normacin, 0.1 mg/mL, fungizone, 2.5 $\mu\text{g}/\text{mL}$ and gentamycin 50 U/mL) and 5% FBS. They were then rinsed with PBS (x2), followed by PBS plus 10 mM dithiothreitol, before being transferred to ice-cold chelation media (PBS plus 8 mM ethylenediaminetetraacetic acid, pH

7.5). Following 60 minutes of incubation on ice in the chelation media, the samples were transferred to fresh PBS containing 5% FBS (Gibco®, Thermo Fisher Scientific, NZ) and shaken vigorously to dislodge the crypts. The tissues were allowed to settle and the supernatant containing the crypts collected. This was repeated until shaking failed to release further crypts. The crypts were then pelleted (40 g, 2 min, 4°C), rinsed in basic culture media (DMEM/F12 containing penicillin [100 U/mL]/streptomycin [100 $\mu\text{g}/\text{mL}$] and 5% FBS). They were then suspended in Matrigel, transferred to 24-well plates (Thermo Fisher Scientific, Waltham, MA), and incubated at 37°C for 10 minutes to polymerize the Matrigel. The crypts were then overlaid with the stem cell culture media (Table 1) and maintained at 37°C in a 5% CO_2 /air mix. The initial structures that develop have a poorly differentiated squamous epithelium and are referred to as colonospheres.⁴⁴ By days 4 to 6, these structures differentiate into columnar epithelial colonoids and cultures consist primarily of differentiated colonoids by days 12 to 14. The culture media was replaced every 48 hours and the colonoids amplified by passaging every 7 days. When amplifying organoids, 10 μM ROCK inhibitor (Merck, Kenilworth, NJ, USA) was included in the growth media. During experiments, this was omitted. All experiments used colonoids (\geq day 12) from passage 2 to 8 only.

Measurement of FITC Flux in Human Intestinal Colonoids

Colonoids from patients were amplified from the initial biopsy so that 4 wells were available from each patient at the same passage. After 12 days of culture, 2 wells of colonoids served as controls while IFN- γ (50 ng/mL) was added to the 2 remaining wells. Six hours after the addition of IFN- γ , tofacitinib (16.7 μM) was added to 1 of the control wells and to 1 of the wells to which IFN- γ had been added. A further addition of tofacitinib (16.7 μM) was made at 24 hours and 48 hours.

The relative permeability of the colonoids was measured by adding 0.1 mg/mL of FD4 to the growth media and measuring the FD4 flux into colonoids with well-developed columnar epithelium 24 hours later. The fluorescence intensity in the midpoint of the organoid lumen was determined by carrying out a series of optical slices through each organoid using a Zeiss 710 LSM confocal microscope (GmbH, Jena, Germany) as previously described.⁴⁵ The fluorescence intensity was then converted to concentration using standard curves created from log serial dilutions of FD4 in growth media. Surface area and volume of the colonoids were calculated from the measured radius to allow calculation of the FD4 flux ($\text{ng}/\text{cm}^2\cdot\text{h}$).

Statistical Analysis

Data are presented as means \pm SEM or fold change from untreated controls for a series of n biological replicates or, in

TABLE 1. Human Colonoid Culture Media Components

Reagent	Stock Conc.	Final Conc.	μl per 50 ml	Supplier	Catalog No.
N2	100X	1X	250	Invitrogen	#17502048
B27	50X	1X	500	Invitrogen	#17504044
Nicotinamide	250 mM	10 mM	1000	Sigma	#N0636
N-acetyl-L-cysteine	500 mM	1 mM	50	Sigma	#A9165
LY 2157299	1 mM	500 nM	25	AxonMedChem	#1491
SB 202190	1 mM	10 μM	250	Sigma	#S7067
PGE ₂	10 μM	0.01 μM	25	Sigma	#P0409
hu EGF	100 μg/mL	50 ng/mL	12.5	Invitrogen	#PHG0311
Noggin	100 μg/mL	100 ng/mL	25	PeptoTech	#120-10C
Gastrin	1 mg/mL	1 μg/mL	25	Pharmaco	3006/1
Wnt3A conditioned media		50%	25,000		
Rspo conditioned media		10%	5000		
Advanced DMEM/F12			17,037.5	Invitrogen	#12634-010
Glutamax	100X (200 mM)	1X	250	Invitrogen	25030-081
Hepes	1M	10 mM	250	Sigma	#H0887
Pen/Strep		1%	250	Invitrogen	15140-122
_a gentamycin	10 mg/mL	50 μg/mL	N/A	Invitrogen	15710064
_a fungizone	250 μg/mL	0.25–2.5 μg/mL	N/A	Invitrogen	109434.01
Normocin	50 mg/mL	0.1 mg/mL	50	Integrated Science	ant-nr-1
_b ROCK inhibitor	1 mM	10 μM	N/A	Merck	#688000-1mg

_aReagents were added in the media only during sample collection. _bReagents were added only when passaging colonoids.

the case of colonoids, patients. Statistical analysis was performed by one-way analysis of variance (ANOVA) and either the Tukey or Newman-Keuls post-test using GraphPad Prism 6 software (GraphPad Software, La Jolla, CA). *P* values ≤ 0.05 were considered statistically significant.

RESULTS

Acute Treatment of Tofacitinib Restricts IFN-γ Activation of JAK1-STAT1/3 Signaling in Intestinal Epithelial Cells

To confirm that tofacitinib was capable of interrupting phosphorylation of JAK1 and its downstream target (STAT1) by IFN-γ in IECs, T₈₄ cells grown in regular 6-well plates were treated with vehicle DMSO or tofacitinib for 1 hour before exposure to IFN-γ for 30 minutes (for JAK1 activation) or 1 hour (for STAT activation) (schematic shown in Fig. 1A). Whole-cell protein lysates were collected, subjected to Western blotting and probed for the proteins indicated. Although the decrease in JAK1 phosphorylation in resting cells treated with tofacitinib did not reach statistical significance, tofacitinib (50 μM) pretreatment significantly reduced IFN-γ-induced JAK1 phosphorylation in T₈₄ cells (*P* < 0.05, *n* = 3; Fig. 1B). As a downstream target of JAK1, STAT1 phosphorylation levels were significantly reduced by acute treatment of tofacitinib compared with

untreated cells and completely blocked IFN-γ-induced STAT1 phosphorylation (*P* < 0.001, *n* = 3; Fig. 1C). Similar results were observed with the phosphorylation levels of STAT3, another mediator of JAK signaling (*P* < 0.05, *P* < 0.001, *n* = 4; Fig. 1D). These data indicate that, in vitro, tofacitinib can prevent cytokine-induced JAK-STAT activation in IECs.

Tofacitinib Prevents IFN-γ-Induced Barrier Dysfunction in Intestinal Epithelial Cells In vitro

IFN-γ is known to disrupt IEC tight junction composition and increase paracellular permeability to electrolytes and macromolecules.^{23, 46} To test whether tofacitinib protected against IFN-γ-stimulated increases in permeability, T₈₄ IECs were grown on transwells and apically treated with tofacitinib or vehicle (DMSO) with or without subsequent basolateral treatment with IFN-γ, (schematic shown in Fig. 2A). After 24 hours, there was no significant difference in TER between untreated, DMSO-treated and cells treated with tofacitinib alone at increasing concentrations of 2 μM, 10 μM and 50 μM (Fig. 2B). While IFN-γ decreased TER, this was unaltered by DMSO. However, tofacitinib prevented the IFN-γ-induced decrease in TER in a dose-dependent manner (*P* < 0.001, *P* < 0.0001, *n* = 3; Fig. 2B). In addition, tofacitinib pretreatment prevented

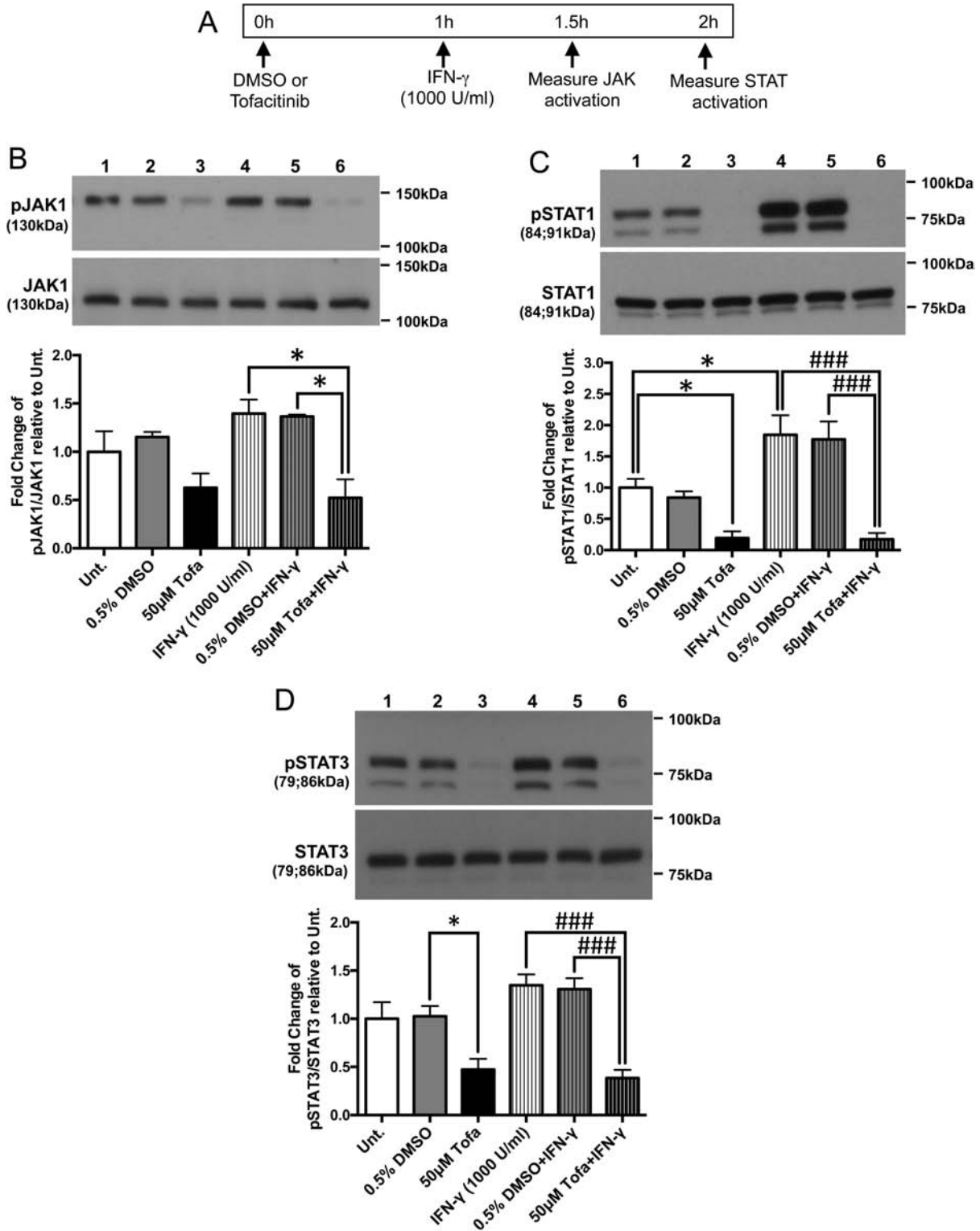


FIGURE 1. Tofacitinib pretreatment prevented IFN- γ -induced JAK1, STAT1, and STAT3 phosphorylation in IECs in vitro. A, Schematic of the acute prevention protocol for tofacitinib to determine JAK-STAT activation in IECs. T₈₄ IECs were treated with vehicle (DMSO) or tofacitinib (Tofa, 50 μ M) for 1 hour followed by IFN- γ (1000 U/mL) treatment for either 30 minutes (for JAK activation) or 1 hour (for STAT activation). Cells were lysed and protein extracts were subjected to Western blotting for the proteins indicated. Densitometric analysis was performed and normalized to (B) pJAK1/JAK1, (C) pSTAT1/STAT1, and (D) pSTAT3/STAT3 levels of each replicate's respective untreated (Unt.) controls (* $P < 0.05$, ### $P < 0.001$, $n = 3-4$).

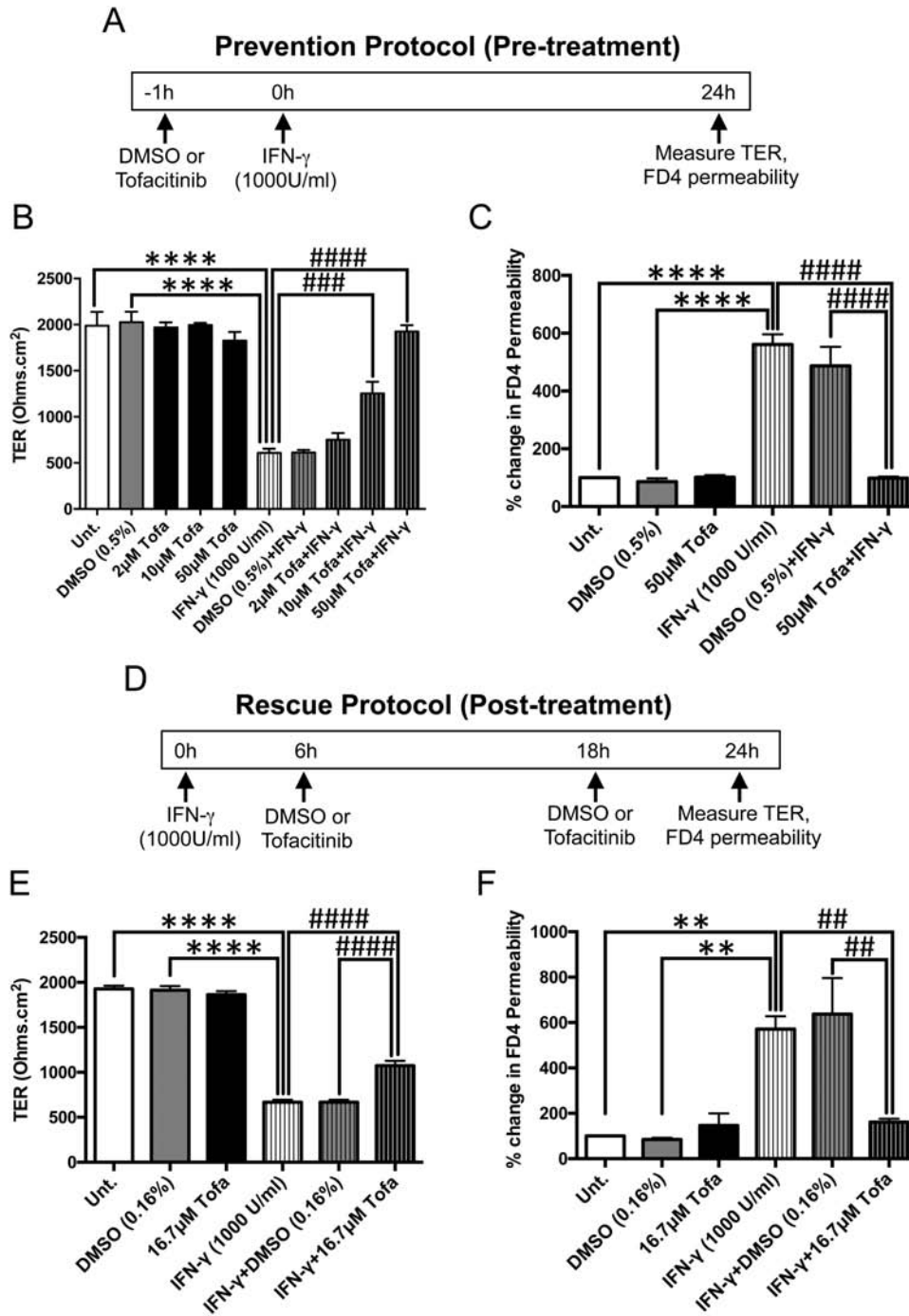


FIGURE 2. Tofacitinib prevents and rescues IECs against IFN- γ -induced barrier dysfunction. A, Schematic of the prevention protocol (pretreatment): T₈₄ IECs grown on transwells were treated with varying concentrations of tofacitinib apically for 1 hour followed by basolateral administration of IFN- γ (1000 U/ml) for 24 hours. DMSO was used as a vehicle control. (B) TER and (C) FD4 permeability were measured 24 hours post-IFN- γ . (**** $P < 0.0001$, ### $P < 0.001$, ##### $P < 0.00001$, $n = 3$). D, Schematic of the rescue protocol (post-treatment): therapeutic effects of tofacitinib were studied by treating T₈₄ IECs post-IFN- γ treatment (1000 U/ml) with tofacitinib (16.7 μ M) apically at 2 time points (6 h and 18 h) to mimic twice daily clinical administration. Again, DMSO was used as a vehicle control. E, TER and (F) FD4 permeability were measured 24 hours after IFN- γ treatment. (**** $P < 0.0001$, ** $P < 0.01$, ##### $P < 0.00001$, ## $P < 0.01$, $n = 3$).

the IFN- γ -induced increase in FD4 permeability compared with DMSO pretreated cells ($P < 0.0001$; $n = 3$; Fig. 2C). Moreover, DMSO or tofacitinib alone had no effect on

FD4 permeability. These results indicate that tofacitinib exerts a protective effect against cytokine-induced paracellular permeability to electrolytes and macromolecules.

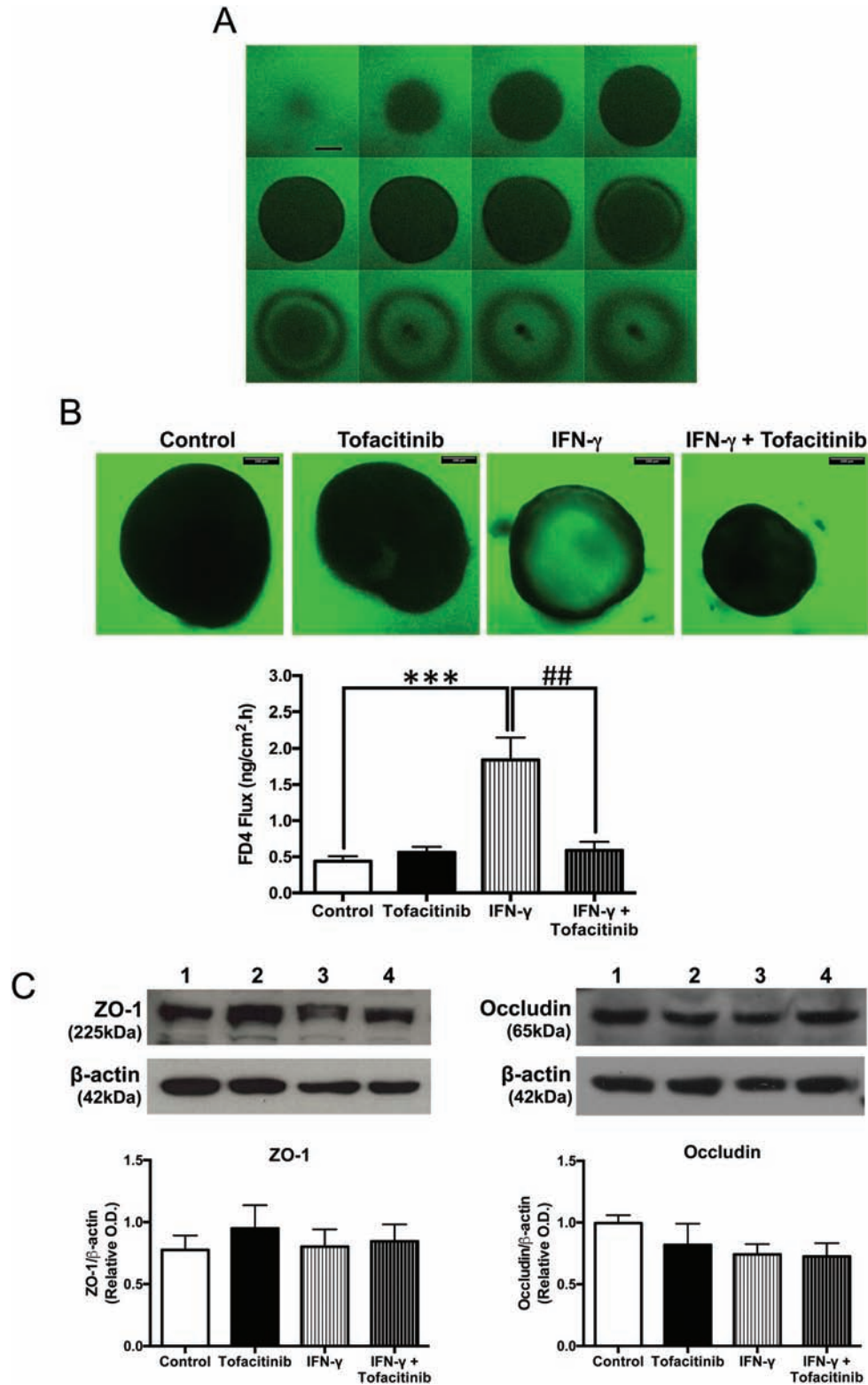


FIGURE 3. Tofacitinib rescues the permeability increase induced by IFN- γ in human colonic organoids. A, Representative series of optical slices through a human colonoid bathed in growth media containing 0.1 mg/mL FD4. Scale bar = 100 μ m. B, Following a rescue protocol, human colonoids cultured for 12 days were treated with IFN- γ (50 ng/mL, administered in the bathing media). Tofacitinib (16.7 μ M, administered in the bathing media) was added 6 hours, 24 hours, and 48 hours post-IFN- γ treatment. FD4 flux across colonoid epithelium normalized to surface area of colonoids was measured 72 hours after IFN- γ administration. (** $P < 0.001$, ## $P < 0.01$, $n = 4$). C, Colonoids were harvested, lysed, and subjected to Western blotting for ZO-1 and occludin. Representative blots and densitometric analysis for ZO-1 and occludin are shown.

Early Intervention with Tofacitinib Partially Rescues the Drop in TER but Fully Restores the Increase in FD4 Permeability Induced by IFN- γ in IECs In Vitro

To test the therapeutic effects of tofacitinib on barrier function, polarized T₈₄ IECs grown on transwells were first treated with basolateral IFN- γ (1000 U/mL) followed by 2 apical doses of tofacitinib (16.7 μ M each) or vehicle DMSO at 2 time points (6 hours and 18 hours post-IFN- γ treatment) to mimic twice daily clinical administration (schematic shown in Fig. 2D). Twenty-four hours after IFN- γ treatment, TER and FD4 permeability were measured. Again, there were no differences in TER between untreated cells and cells treated with either DMSO or tofacitinib alone. However, the drop in TER induced by IFN- γ , which was unaffected by DMSO, was partially restored by tofacitinib ($P < 0.0001$, $n = 3$; Fig. 2E). Moreover, the increase in FD4 permeability induced by IFN- γ was fully rescued by treatment with tofacitinib ($P < 0.01$, $n = 3$; Fig. 2F). These data suggest that early intervention of tofacitinib is able to differentially rescue modes of IFN- γ -induced barrier dysfunction.

Tofacitinib Reverses the FD4 Permeability Increase Induced by IFN- γ in Human Colonic Organoids

Human colonic enteroids (colonoids) have a mature columnar epithelium which contains both a stem cell niche and other differentiated cell types surrounding a single luminal compartment. To more accurately reflect the complex three-dimensional structure of the intestinal epithelium, human colonoids were used to determine the effect of tofacitinib on permeability. Figure 3A shows a representative panel of optical slices through 1 colonoid, the midpoint of which is where FD4 signal intensity was measured. Supplementary Figure 1 illustrates how the optical slices of the organoids were obtained and depicted. After 72 hours, IFN- γ treatment resulted in a 3- to 4-fold increase in FD4 influx into the colonoids from the bathing media, as shown in Figure 3B. The addition of tofacitinib rescued the IFN- γ -induced increase in FD4 flux while yielding no effect on the basal flux ($P < 0.01$, $n = 4$; Fig. 3B). Changes in expression of tight junction proteins regulating the leak pathway can alter paracellular FD4 permeability across a monolayer of intestinal cells.²³ To better understand if changes in FD4 permeability seen in Figure 3B were due to altered tight junction protein expression, colonoids were harvested and processed for Western blotting. Figure 3C shows that the protein expression of ZO-1 and occludin were unaltered in organoids subjected to these treatments.

Similar to observations seen in human organoids, none of the treatment conditions had a significant impact on the protein expression of ZO-1, occludin, or another transmembrane MARVEL family protein, tricellulin, in T₈₄ monolayers

subjected to the treatments in Figure 2A and D ($n = 4$; Fig. 4). These results imply that the effects of IFN- γ and tofacitinib on FD4 permeability across the epithelium are likely not due to alterations in the expression of these tight junction proteins.

Tofacitinib Protects the Epithelial Barrier by Restricting IFN- γ -Induced ZO-1 Relocalization

After we ruled out changes in tight junction protein expression by tofacitinib, to determine the mechanism(s) behind the protective effects of tofacitinib against the IFN- γ -induced increase in FD4 permeability seen in Fig. 2C, T₈₄ cells seeded on glass coverslips were treated with tofacitinib or DMSO for 1 hour, followed by IFN- γ treatment for 24 hours. Assessment of ZO-1 staining in fixed cells revealed that IFN- γ treatment caused increased formation of intercellular gaps that disrupted the regular chickenwire pattern seen in untreated and DMSO-treated cells (Fig. 5A). The intercellular gaps were observed less frequently in cells pretreated with tofacitinib, as quantified in Figure 5B. Similar observations were seen in cells treated with tofacitinib 6 hours and 18 hours post-IFN- γ challenge (Fig. 5C) as quantified in Figure 5D. In staining for occludin in IFN- γ -treated cells, z-stack imaging revealed that these intercellular gaps were restricted to the apical portion of the cell monolayer and did not span the height of the IECs. A representative movie of a gap, assessed by membrane occludin staining through z-stack imaging, is shown in the supplementary material online, which confirms apical localization of the gap. These data suggest that the beneficial effects of tofacitinib in reducing FD4 permeability in this model system are likely due to normalizing localization of TJ proteins, including ZO-1, rather than by affecting their overall expression.

Tofacitinib Restricts IFN- γ -Induced Claudin-2 Promoter Activity and Protein Expression

To identify the mechanism(s) by which tofacitinib reduced the drop in TER caused by IFN- γ treatment, protein lysates were collected from polarized T₈₄ IECs treated with tofacitinib or DMSO with or without IFN- γ exposure using the “prevention” and “rescue” protocols described in Figures 2A and D, respectively. Lysates were then subjected to Western blotting and probed for the expression of the cation selective pore-forming tight junction protein, claudin-2. After 24 hours, IFN- γ increased claudin-2 levels more than 2-fold from untreated and DMSO-treated controls ($P < 0.001$, $n = 3$; Fig. 6A). Conversely, tofacitinib pretreatment prevented the IFN- γ -induced increase in claudin-2 protein levels in vitro ($P < 0.05$, $n = 3$; Fig. 6A). When administered after IFN- γ exposure, tofacitinib could only partially normalize claudin-2 protein levels ($P < 0.05$, $n = 3$; Fig. 6B). To identify the mechanism of claudin-2 upregulation affected by tofacitinib, we examined its effects on claudin-2 gene transcription given that the claudin-2 promoter contains a STAT-binding motif. We previously demonstrated in HT-29

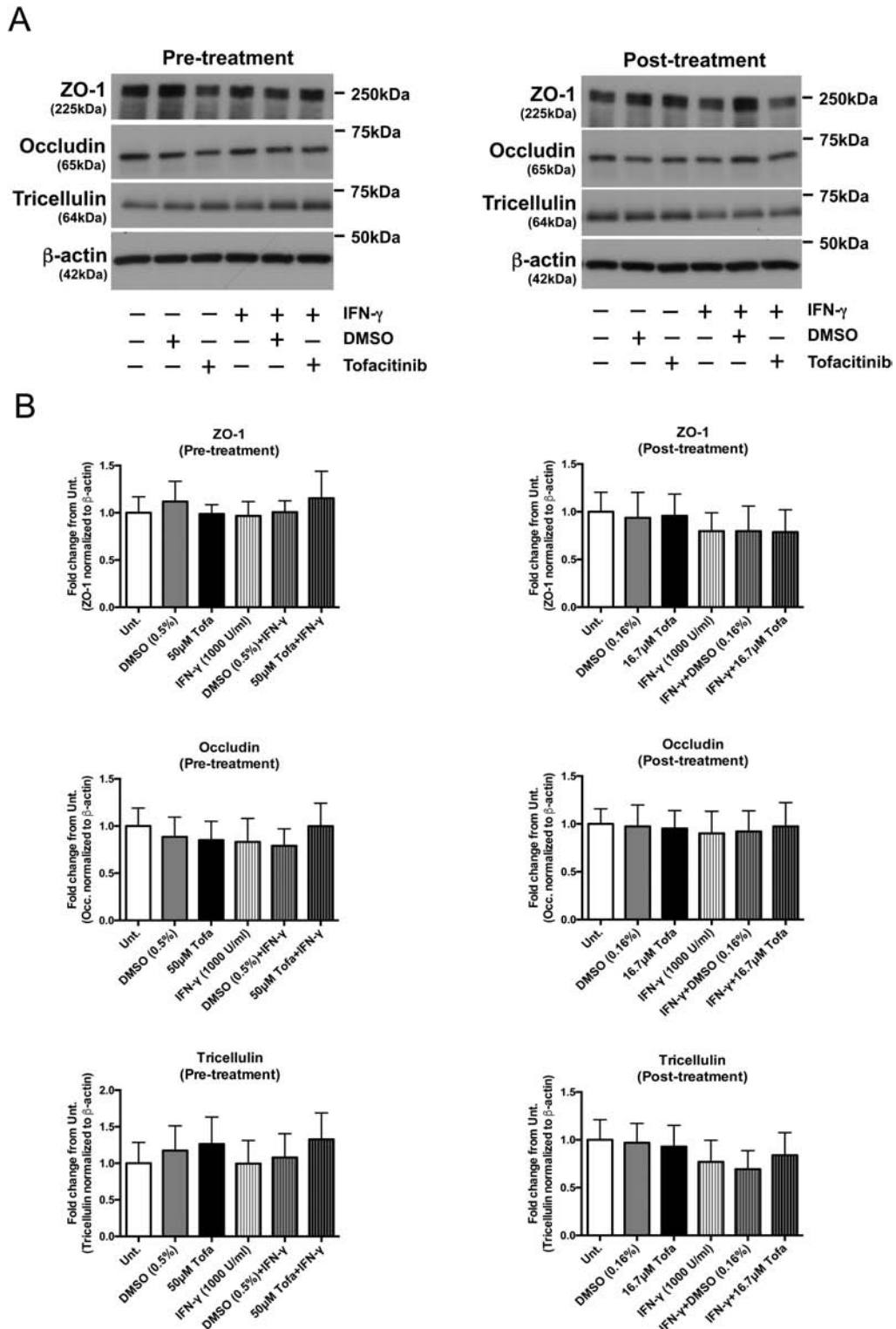


FIGURE 4. Tofacitinib does not alter protein expression of tight junction proteins involved in macromolecule permeability. Pretreatment: T₈₄ cells grown in transwells were pretreated with DMSO or tofacitinib (50 µM) for 1 hour before IFN- γ (1000 U/mL) treatment for 24 hours. Post-treatment: T₈₄ cells grown in transwells were first treated with IFN- γ (1000 U/mL) followed by 2 doses of DMSO or tofacitinib (16.7 µM) at 6 hours and 18 hours post-IFN- γ administration. Twenty-four hours after IFN- γ exposure, cells were lysed, processed for Western blotting, and probed for the proteins indicated. A, Representative blots probed for ZO-1, occludin, tricellulin, and β actin. B, Quantification of densitometric analysis normalized to untreated controls from 4 independent experiments ($n = 4$).

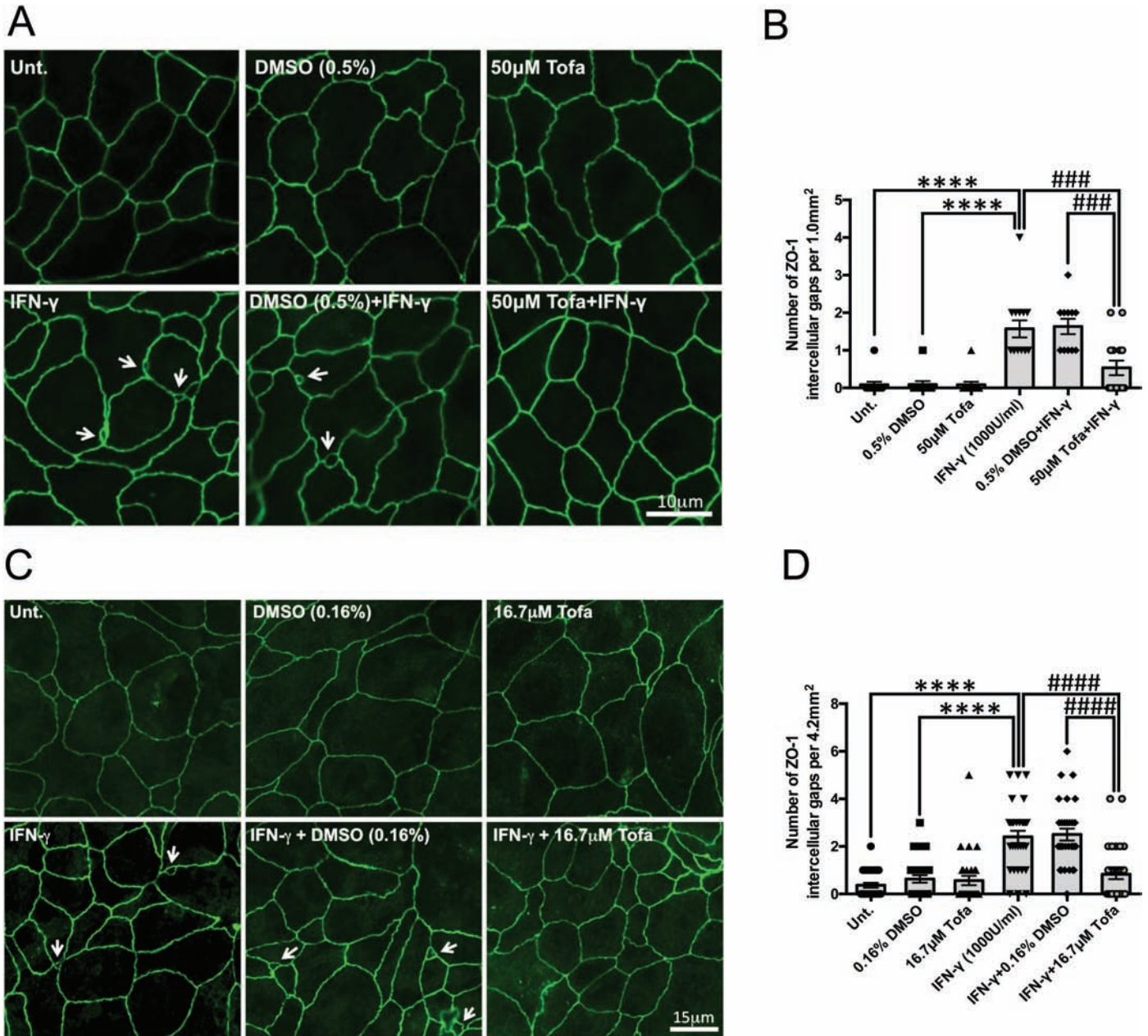


FIGURE 5. Tofacitinib reduces the number of apical intercellular gaps via ZO-1 rearrangement/localization caused by IFN- γ . A, Pretreatment: T₈₄ cells grown on coverslips pretreated with tofacitinib or DMSO for 1 hour followed by IFN- γ (1000 U/mL, 24 h) treatment were stained for ZO-1 and visualized via immunofluorescence microscopy. B, Average number of intercellular gaps in 5 fields of view per condition from 3 independent pretreatment experiments (**** $P < 0.0001$, ### $P < 0.001$, ## $P < 0.01$, $n = 3$). C, Post-treatment: ZO-1 staining in cells treated with tofacitinib or DMSO at 6 hours and 18 hours post-IFN- γ (1000 U/mL, 24 h) treatment. D, Number of intercellular gaps taken in 10 fields of view per condition from 3 independent post-treatment experiments (**** $P < 0.0001$, ### $P < 0.001$, $n = 3$). White arrows indicate intercellular gaps.

IECs expressing a claudin-2 promoter-luciferase construct that following IFN- γ treatment, STAT1 binds to the claudin-2 promoter to induce its transcription.¹⁵ In this study, HT-29 cells pretreated with tofacitinib 1 hour before IFN- γ exposure for 24 hours displayed reduced claudin-2 promoter activity compared with cells challenged with IFN- γ alone or pretreated

with DMSO ($P < 0.001$, $n = 4$; Fig. 6C). The tofacitinib-induced changes in claudin-2 protein levels suggest that tofacitinib reduces the changes in TER induced by IFN- γ —at least in part—through claudin-2 regulation. In addition to claudin-2, other members of the claudin family also contribute to changes in TER across an epithelium. Claudin-1 and claudin-4 are known

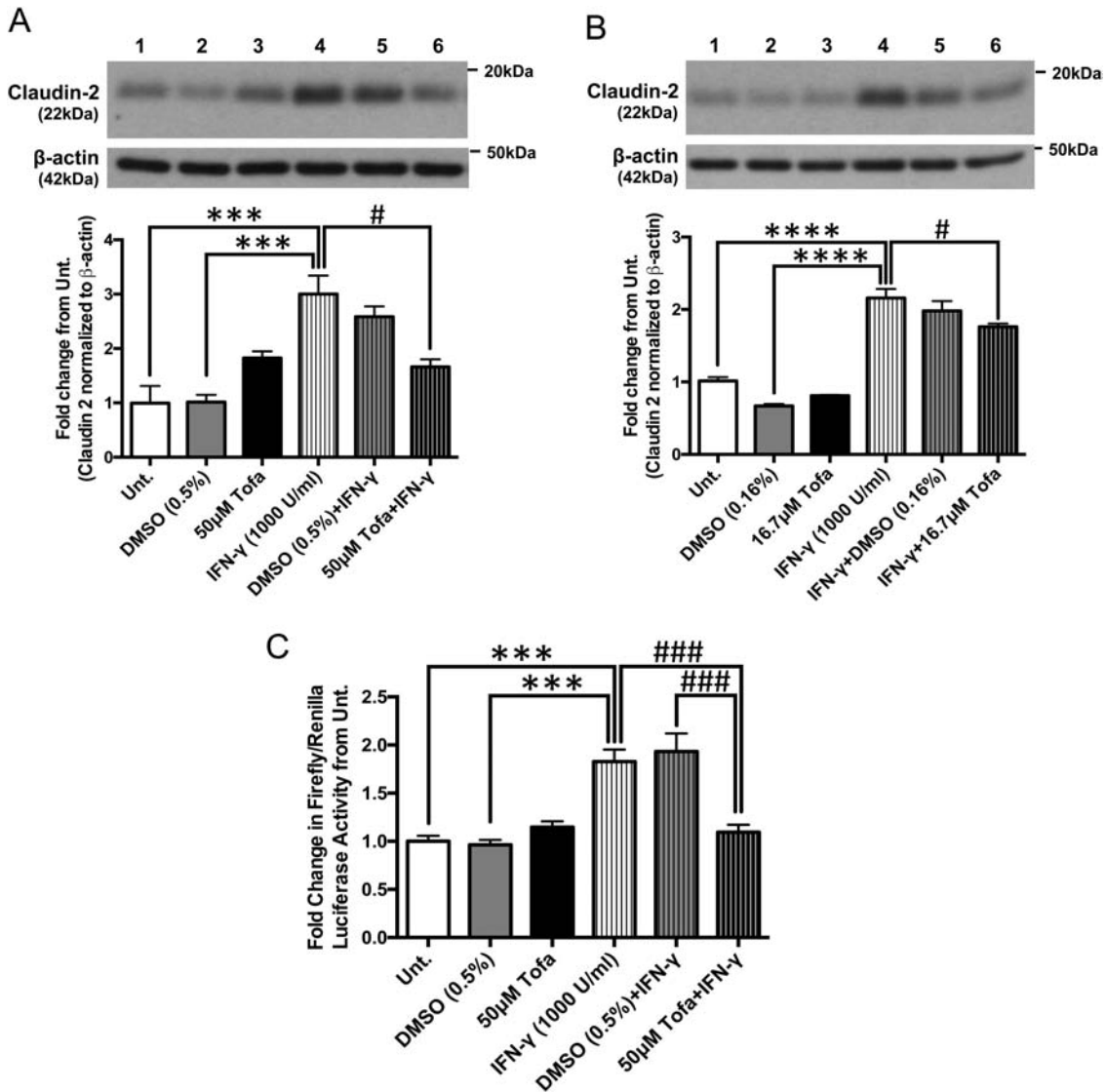


FIGURE 6. Tofacitinib restricts IFN-γ-induced claudin-2 protein expression and promoter activity. A, Pretreatment: claudin-2 protein expression was determined in T₈₄ IECs pretreated with tofacitinib or DMSO 1 hour before IFN-γ treatment for 24 hours and quantified using densitometric analysis and normalized to untreated controls. (***) $P < 0.001$, # $P < 0.05$, $n = 4$). B, Post-treatment: claudin-2 protein expression was determined in T₈₄ cells treated with tofacitinib or DMSO 6 hours and 18 hours post-IFN-γ exposure and quantified using densitometric analysis and normalized to untreated controls. (****) $P < 0.0001$, # $P < 0.05$, $n = 3$). C, Pretreatment: claudin-2 promoter activity was measured using a luciferase reporter assay on HT-29 IECs subjected to the treatment schedule outlined in Figure 1A. (***) $P < 0.001$, ### $P < 0.001$, $n = 4$).

to tighten the barrier and increase TER, whereas overexpressing claudin-15 decreases TER and increases paracellular flux of cations, similar to claudin-2.⁵⁴ However, protein expression of these claudins did not significantly change with tofacitinib or IFN-γ treatments (Supplementary Fig. 2), thus suggesting that the effects seen in TER are most likely mediated by the changes in claudin-2 expression.

DISCUSSION

Tofacitinib is a selective inhibitor of members of the JAK family kinases and demonstrates strong selectivity for

JAK1 and JAK3 >>> JAK2 > tyrosine kinase 2 (TYK2).³⁸ By inhibiting JAK phosphorylation, tofacitinib inhibits recruitment of downstream STAT family members by activated JAK1 and thus interrupts these signaling cascades, thereby reducing STAT-dependent activation of inflammatory genes (Fig. 7).^{30, 38} Tofacitinib has proven to be an effective therapeutic agent in treating several chronic inflammatory diseases and has been FDA-approved for the treatment of rheumatoid arthritis, psoriasis, and more recently, ulcerative colitis.³⁹ In phase 2 clinical trials, remission at 52 weeks occurred in up to 40.6% of UC patients who received 10 mg of tofacitinib twice daily, compared

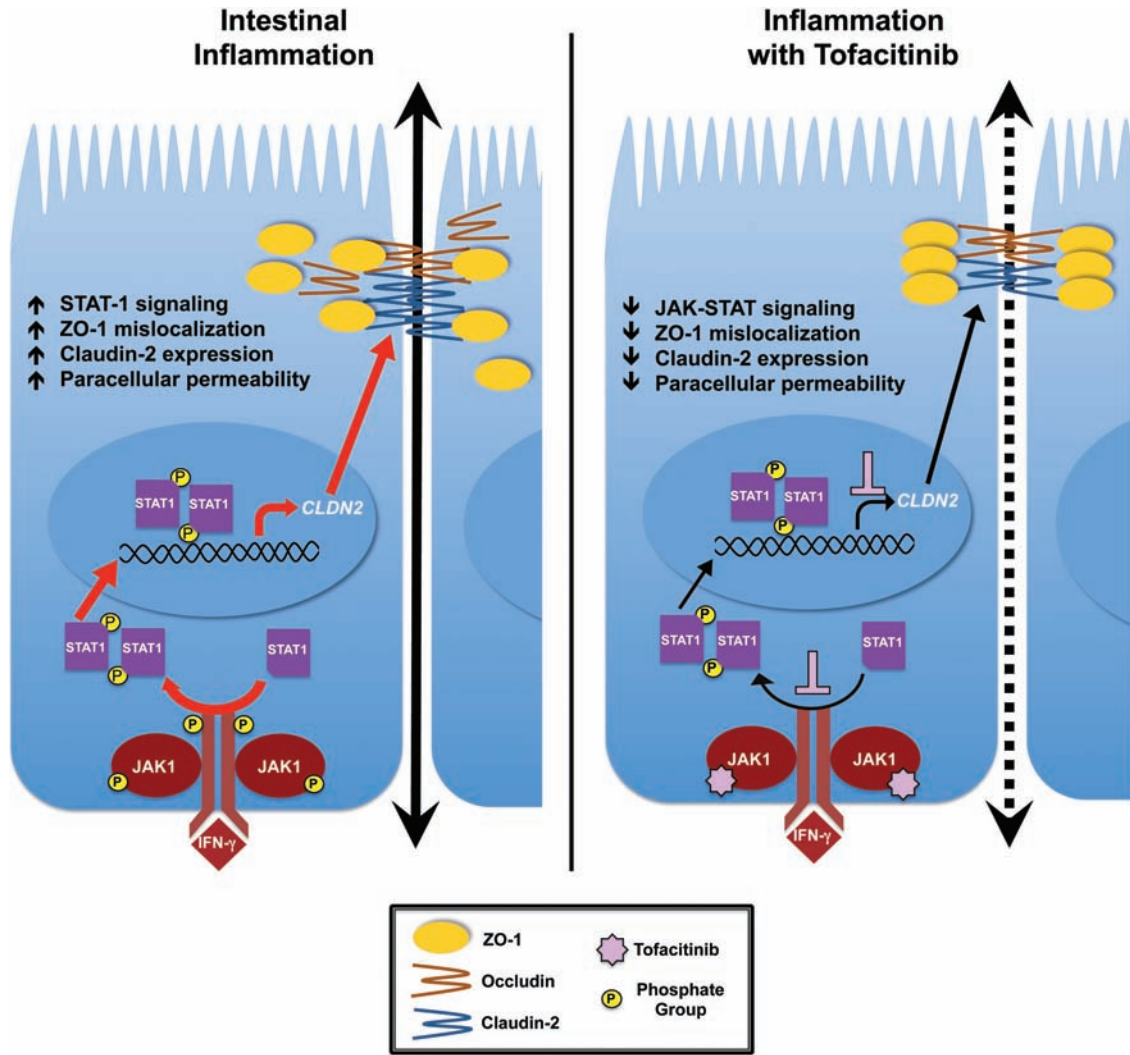


FIGURE 7. The protective effect of tofacitinib on IFN- γ -induced barrier dysfunction. During inflammation in which cytokines such as IFN- γ are released and bind to their receptors on epithelial cells, JAK1 proteins are brought in close proximity to each other and are activated. These in turn phosphorylate cytokine receptors that serve as docking sites for STAT proteins, which are then activated by JAK1 proteins. Phosphorylated STATs dimerize, translocate to the nucleus, and serve as transcription factors for specific genes, such as claudin-2. Upon IFN- γ treatment, claudin-2 expression is upregulated and ZO-1 mislocalizes to form intercellular gaps. As a small molecule inhibitor, when tofacitinib binds to the ATP-binding site of JAK proteins, the first step of the signaling cascade is stopped, therefore preventing and/or reducing the detrimental effects of IFN- γ on the intestinal epithelial barrier (summarized in right-hand panel; broken arrow reflects reduced paracellular permeability vs. inflammation alone shown in left-hand panel).

with 11.1% in the placebo group.³⁹ At the same time, mucosal healing at 52 weeks occurred in 45.7% of patients on tofacitinib compared with 13.1% in those receiving placebo.^{39, 47} Although one of the primary endpoints of this study was mucosal healing, the direct effects of tofacitinib on the critical mucosal cell type comprising the intestinal barrier is unknown.

In this study, we show that tofacitinib exerts a direct effect on IECs *in vitro* by inhibiting cytokine-induced JAK1-STAT1/3 activation. The timing of IFN- γ exposure was optimized for either maximal JAK1 or STAT1/3 phosphorylation and

tofacitinib reduced IFN- γ stimulated pJAK1, pSTAT1 and pSTAT3 to levels comparable to controls. Moreover, tofacitinib not only was capable of preventing permeability increases caused by IFN- γ but also rescued epithelial monolayers from IFN- γ -induced increases in barrier permeability. Treating IECs with tofacitinib before the IFN- γ challenge prevented the dramatic decrease in TER and FD4 permeability enhancement. This suggests that tofacitinib inhibition of JAKs before exposure to a pro-inflammatory mediator is sufficient to maintain the barrier's integrity. This may have relevance to the clinical

efficacy of tofacitinib in potentially limiting the epithelial barrier-disrupting effects of newly secreted inflammatory cytokines at the start of a flare in disease activity. The capacity of tofacitinib to rescue the permeability defect caused by IFN- γ in primary human colonoids further supports the evidence of a direct beneficial effect of tofacitinib on the intestinal epithelium. Human colonoids better recapitulate the microenvironment of IECs as they are grown in 3-dimensional orientation, thus retaining both the structure and variety of epithelial cell subtypes of the colonic crypt.^{48–51} Of note, though the same concentration of tofacitinib used for cell culture studies was able to rescue the increase in FD4 permeability caused by IFN- γ in colonoids, this was studied over a longer time period of exposure in colonoids than cell lines. Collectively, these data indicate that tofacitinib rescued barrier function using both epithelial model systems, thus further validating the efficacy of this agent in normalizing barrier function.

We have attempted to discriminate between the 2 principal forms of permeability that are regulated by specific tight junction alterations, namely the size- and charge-selectivity of electrolyte flux as measured by TER (pore pathway) and the size but noncharge-selective permeability characterized by FD4 permeability (leak pathway).⁵² Although increased involvement of the leak pathway can also lead to a reduction in TER, this functional parameter of permeability often correlates with changes in the expression of claudin family proteins, with increased expression of claudin-2 contributing directly to reduced TER due to increased flux of Na⁺ and water.^{9, 11, 14, 53–55} We previously demonstrated that STAT1 binding is partly responsible for the IFN- γ -induced increase in claudin-2 promoter activity, and mutation of the STAT-binding domain eliminates IFN- γ -induced *CLDN2* promoter activity.¹⁵ Our current data indicate that the inhibitory effect of tofacitinib on claudin-2 upregulation is at least partly attributed to inhibition of the *CLDN2* promoter (Fig. 7). In agreement with our previous findings, this inhibitory effect is likely due to reduced STAT1-mediated transcription of claudin-2 since STAT1 is a substrate of activated JAK1. Even though we previously demonstrated that STAT1 binds to the *CLDN2* promoter to increase *CLDN2* expression via a STAT-binding motif, involvement of other STATs—specifically STAT6 in the regulation of claudin-2 expression by the inflammatory cytokine IL-13—has also been demonstrated.^{14, 15, 56–58} However, our data do contrast with prior studies indicating that pharmacological inhibitors of STAT1 were unable to alleviate the IFN- γ -induced reduction in TER.^{37, 59–61} Data from the same group suggested that following IFN- γ treatment, STAT1 promoted STAT5b activation, which formed a complex with Fyn Src kinase and PI 3-kinase to serve as a mediator of IFN- γ -induced barrier dysfunction, specifically macromolecule horseradish peroxidase translocation in T₈₄ monolayers.⁵⁶ These studies highlight how STAT proteins have versatile and complex roles in barrier function regulation, which can be context-dependent.

IFN- γ is a recognized modulator of the tight junction localization and expression of occludin and ZO-1.^{15, 32–36, 62} In the present study, we did not observe a significant difference in the expression levels of ZO-1, occluding, or another member of the MARVEL family of transmembrane proteins involved in restricting macromolecular permeability, tricellulin, after IFN- γ treatment for 24 hours.^{16–18} This suggests that the IFN- γ -induced increase in FD4 permeability—and thus the normalizing effect of tofacitinib on FD4—are likely not mediated by changes in overall protein expression of ZO-1, occludin, or tricellulin. Instead, the inhibitory effect of tofacitinib on FD4 permeability is likely due to changes in tight junction protein localization. This was supported by ZO-1 relocation data and the decreased frequency of intercellular gaps observed with ZO-1 immunofluorescence-staining in cell monolayers treated with tofacitinib. Indeed, IFN- γ -induced alterations in barrier permeability and tight junction protein relocation may partially be due to remodeling or internalization of these tight junction proteins from the plasma membrane into a subapical cytosolic compartment, as previously described.³⁶

Our study also showed that early intervention with tofacitinib during exposure to IFN- γ can fully rescue the increase in FD4 permeability, yet only partially mitigate the decrease in TER. This partial restoration correlates with our finding that claudin-2 protein expression levels did not return to those of untreated and DMSO-treated controls in the rescue protocol studies. A potential explanation could be that tofacitinib is unable to fully reverse the sequence of signaling events leading to increased claudin-2 and TER loss as opposed to its apparent capacity to arrest signaling modalities targeting junction proteins involved in the leak barrier defect and thus reverse the increase in FD4 permeability caused by IFN- γ .

The concentration of tofacitinib used here to study barrier and JAK/STAT signaling effects on IECs are relatively higher compared with those used in other studies. For instance, tofacitinib at 30 nM and 100 nM reduced cytokine-induced STAT1 phosphorylation in CD4⁺ T cells and fibroblast-like synoviocytes, respectively.^{63, 64} However, this discrepancy could be attributed to the different cell types studied, as in our experience intestinal epithelial cell lines are not as sensitive to inflammatory cytokines or pharmacological inhibitors as other cell types. Moreover as shown in Figure 2B, the lowest dose of 2 μ M of tofacitinib did not produce a barrier-protecting effect against IFN- γ in IEC monolayers, suggesting that in this experimental system, higher concentrations of tofacitinib are required to modulate downstream effector responses in readouts such as barrier function. Of note however, in our studies tofacitinib was administered at 2.6 mg (16.7 μ M) or 7.8 mg (50 μ M), which is within the dosage range of 5 or 10 mg given to ulcerative colitis patients.^{39, 65}

CONCLUSIONS

In summary, we have demonstrated that the JAK inhibitor tofacitinib is capable of both protecting against and rescuing from the deleterious effects of IFN- γ on intestinal epithelial permeability using both cell line and human organoid model systems. Patients with ulcerative colitis who received tofacitinib for 8 weeks had significantly higher clinical response rates and lower Mayo endoscopic subscores compared with those receiving placebo.^{39, 47, 65} Additionally, those who received tofacitinib had higher remission rates at 52 weeks compared with those receiving placebo.³⁹ Our results suggest that part of the clinical benefits of tofacitinib in treating ulcerative colitis patients may accrue from reducing the activity of JAK-activated signaling pathways that disrupt tight junction protein composition in IECs. Although tofacitinib has been demonstrated to promote mucosal healing, we propose that part of its efficacy may also lie in its ability to restore normal mucosal barrier function as reflected by the normalization of permeability to macromolecules and reduced electrolyte flux.

SUPPLEMENTARY DATA

Supplementary data is available at *Inflammatory Bowel Diseases* online.

Supplementary Figure 1: Images of colonoids are taken from optical slices of each colonoid. This illustration depicts how the representative panel of optical sections were taken in different planes of one 3D organoid, starting from just above the organoid and finishing below the organoid, thus resulting in differences in diameter of the image.

Supplementary Figure 2: No significant changes in protein expression of claudins 1, 4, and 15 were found with any of the treatments in vitro.

T84 monolayers were subjected to vehicle (DMSO), tofacitinib and IFN- γ treatments following the “prevention” and “rescue” protocols. Cells were lysed, whole-cell protein lysates were processed, subjected to Western blotting, and probed for claudin-1, claudin-4, and claudin-15. ($n = 3-4$).

Supplementary Movie 1: Occludin localization reveals that intercellular gaps induced by IFN- γ are restricted to the apical poles of T₈₄ cell monolayers.

T₈₄ cells grown on glass coverslips treated with IFN- γ (1000 U/mL, 24 h) were fixed and stained for occludin. In IFN- γ -treated cells, z-stack images compiled into this movie show that the intercellular gaps do not span along the lateral side of IECs but rather are restricted to the apical portion of the cell monolayer. The arrow indicates a gap that appears then quickly disappears as the imaging plane moves from the apical to the basolateral portion of the cells. This is a representative movie from 3 independent experiments.

ACKNOWLEDGMENTS

Authors would like to thank Dr. Christian Lytle (University of California Riverside) and Dr. David Lo (UC Riverside)

for technical expertise, thoughtful discussions, and valuable suggestions. They are also grateful to Dr. Djurdica Coss and Dr. Nancy Lainez (UC Riverside) for technical assistance and use of the Promega microplate reader for the FD4 permeability and luciferase reporter assays. They also thank Dr. David Lo and Sarah Miller (UC Riverside) for equipment use and technical assistance with confocal microscopy imaging of occludin staining in IECs. Lastly, they would like to thank the UCR Biomedical Sciences Division for the Pease Cancer Fellowship awarded to AS.

REFERENCES

1. Zeissig S, Bürgel N, Günzel D, et al. Changes in expression and distribution of claudin 2, 5 and 8 lead to discontinuous tight junctions and barrier dysfunction in active Crohn's disease. *Gut*. 2007;56:61–72.
2. Turner JR, Rill BK, Carlson SL, et al. Physiological regulation of epithelial tight junctions is associated with myosin light-chain phosphorylation. *Am J Physiol*. 1997;273:C1378–C1385.
3. Bruewer M, Samarin S, Nusrat A. Inflammatory bowel disease and the apical junctional complex. *Ann N Y Acad Sci*. 2006;1072:242–252.
4. Anderson JM, Van Itallie CM. Tight junctions and the molecular basis for regulation of paracellular permeability. *Am J Physiol*. 1995;269:G467–G475.
5. Anbazhagan AN, Priyamvada S, Alrefai WA, et al. Pathophysiology of IBD associated diarrhea. *Tissue Barriers*. 2018;6:e1463897.
6. Irvine EJ, Marshall JK. Increased intestinal permeability precedes the onset of Crohn's disease in a subject with familial risk. *Gastroenterology*. 2000;119:1740–1744.
7. Olson TS, Reuter BK, Scott KG, et al. The primary defect in experimental ileitis originates from a nonhematopoietic source. *J Exp Med*. 2006;203:541–552.
8. Su L, Shen L, Clayburgh DR, et al. Targeted epithelial tight junction dysfunction causes immune activation and contributes to development of experimental colitis. *Gastroenterology*. 2009;136:551–563.
9. Shen L, Weber CR, Raleigh DR, et al. Tight junction pore and leak pathways: a dynamic duo. *Annu Rev Physiol*. 2011;73:283–309.
10. Clayburgh DR, Shen L, Turner JR. A porous defense: the leaky epithelial barrier in intestinal disease. *Lab Invest*. 2004;84:282–291.
11. Amasheh S, Meiri N, Gitter AH, et al. Claudin-2 expression induces cation-selective channels in tight junctions of epithelial cells. *J Cell Sci*. 2002;115:4969–4976.
12. Prasad S, Mingrino R, Kaukinen K, et al. Inflammatory processes have differential effects on claudins 2, 3 and 4 in colonic epithelial cells. *Lab Invest*. 2005;85:1139–1162.
13. Heller F, Florian P, Bojarski C, et al. Interleukin-13 is the key effector Th2 cytokine in ulcerative colitis that affects epithelial tight junctions, apoptosis, and cell restitution. *Gastroenterology*. 2005;129:550–564.
14. Weber CR, Raleigh DR, Su L, et al. Epithelial myosin light chain kinase activation induces mucosal interleukin-13 expression to alter tight junction ion selectivity. *J Biol Chem*. 2010;285:12037–12046.
15. Krishnan M, McCole DF. T cell protein tyrosine phosphatase prevents STAT1 induction of claudin-2 expression in intestinal epithelial cells. *Ann N Y Acad Sci*. 2017;1405:116–130.
16. Ikenouchi J, Furuse M, Furuse K, et al. Tricellulin constitutes a novel barrier at tricellular contacts of epithelial cells. *J Cell Biol*. 2005;171:939–945.
17. Krug SM, Amasheh S, Richter JF, et al. Tricellulin forms a barrier to macromolecules in tricellular tight junctions without affecting ion permeability. *Mol Biol Cell*. 2009;20:3713–3724.
18. Raleigh DR, Marchiando AM, Zhang Y, et al. Tight junction-associated MARVEL proteins marveld3, tricellulin, and occludin have distinct but overlapping functions. *Mol Biol Cell*. 2010;21:1200–1213.
19. McCole DF. IBD candidate genes and intestinal barrier regulation. *Inflamm Bowel Dis*. 2014;20:1829–1849.
20. Furuse M, Itoh M, Hirase T, et al. Direct association of occludin with ZO-1 and its possible involvement in the localization of occludin at tight junctions. *J Cell Biol*. 1994;127:1617–1626.
21. Nusrat A, Chen JA, Foley CS, et al. The coiled-coil domain of occludin can act to organize structural and functional elements of the epithelial tight junction. *J Biol Chem*. 2000;275:29816–29822.
22. Van Itallie CM, Anderson JM. Occludin confers adhesiveness when expressed in fibroblasts. *J Cell Sci*. 1997;110(Pt 9):1113–1121.
23. Al-Sadi R, Boivin M, Ma T. Mechanism of cytokine modulation of epithelial tight junction barrier. *Front Biosci (Landmark Ed)*. 2009;14:2765–2778.
24. Marchiando AM, Shen L, Graham WV, et al. Caveolin-1-dependent occludin endocytosis is required for TNF-induced tight junction regulation in vivo. *J Cell Biol*. 2010;189:111–126.

25. Van Itallie CM, Fanning AS, Holmes J, et al. Occludin is required for cytokine-induced regulation of tight junction barriers. *J Cell Sci*. 2010;123:2844–2852.
26. Kaser A, Zeissig S, Blumberg RS. Inflammatory bowel disease. *Annu Rev Immunol*. 2010;28:573–621.
27. Jostins L, Ripke S, Weersma RK, et al. Host-microbe interactions have shaped the genetic architecture of inflammatory bowel disease. *Nature*. 2012;491:119–124.
28. Liu JZ, van Sommeren S, Huang H, et al.; International Multiple Sclerosis Genetics Consortium; International IBD Genetics Consortium. Association analyses identify 38 susceptibility loci for inflammatory bowel disease and highlight shared genetic risk across populations. *Nat Genet*. 2015;47:979–986.
29. Fuss IJ, Neurath M, Boirivant M, et al. Disparate CD4+ lamina propria (LP) lymphokine secretion profiles in inflammatory bowel disease. *J Immunol*. 1996;157:1261–1270.
30. Shuai K, Liu B. Regulation of JAK-STAT signalling in the immune system. *Nat Rev Immunol*. 2003;3:900–911.
31. Mudter J, Weigmann B, Bartsch B, et al. Activation pattern of signal transducers and activators of transcription (STAT) factors in inflammatory bowel diseases. *Am J Gastroenterol*. 2005;100:64–72.
32. Penrose HM, Marchelletta RR, Krishnan M, et al. Spermidine stimulates T cell protein-tyrosine phosphatase-mediated protection of intestinal epithelial barrier function. *J Biol Chem*. 2013;288:32651–32662.
33. Watson CJ, Hoare CJ, Garrod DR, et al. Interferon-gamma selectively increases epithelial permeability to large molecules by activating different populations of paracellular pores. *J Cell Sci*. 2005;118:5221–5230.
34. Beaurepaire C, Smyth D, McKay DM. Interferon-gamma regulation of intestinal epithelial permeability. *J Interferon Cytokine Res*. 2009;29:133–144.
35. Bruewer M, Luegering A, Kucharzik T, et al. Proinflammatory cytokines disrupt epithelial barrier function by apoptosis-independent mechanisms. *J Immunol*. 2003;171:6164–6172.
36. Bruewer M, Utech M, Ivanov AI, et al. Interferon-gamma induces internalization of epithelial tight junction proteins via a macropinocytosis-like process. *Faseb J*. 2005;19:923–933.
37. Utech M, Ivanov AI, Samarín SN, et al. Mechanism of IFN-gamma-induced endocytosis of tight junction proteins: myosin II-dependent vacuolarization of the apical plasma membrane. *Mol Biol Cell*. 2005;16:5040–5052.
38. Hodge JA, Kawabata TT, Krishnaswami S, et al. The mechanism of action of tofacitinib - an oral Janus kinase inhibitor for the treatment of rheumatoid arthritis. *Clin Exp Rheumatol*. 2016;34:318–328.
39. Sandborn WJ, Su C, Sands BE, et al.; OCTAVE Induction 1, OCTAVE Induction 2, and OCTAVE Sustain Investigators. Tofacitinib as induction and maintenance therapy for ulcerative colitis. *N Engl J Med*. 2017;376:1723–1736.
40. Panés J, Sandborn WJ, Schreiber S, et al. Tofacitinib for induction and maintenance therapy of Crohn's disease: results of two phase IIb randomised placebo-controlled trials. *Gut*. 2017;66:1049–1059.
41. Pfizer, Inc. *Pfizer Announces U.S. FDA Approves Xeljanz® (tofacitinib) for the Treatment of Moderately to Severely Active Ulcerative Colitis*. 2018. https://www.pfizer.com/news/press-release/press-release-detail/pfizer_announces_u_s_fda_approves_xeljanz_tofacitinib_for_the_treatment_of_moderately_to_severely_active_ulcerative_colitis-0. Accessed April 16, 2018.
42. Schneider CA, Rasband WS, Eliceiri KW. NIH Image to ImageJ: 25 years of image analysis. *Nat Methods*. 2012;9:671–675.
43. Sato T, Stange DE, Ferrante M, et al. Long-term expansion of epithelial organoids from human colon, adenoma, adenocarcinoma, and Barrett's epithelium. *Gastroenterology*. 2011;141:1762–1772.
44. Stelzner M, Helmrath M, Dunn JC, et al.; NIH Intestinal Stem Cell Consortium. A nomenclature for intestinal in vitro cultures. *Am J Physiol Gastrointest Liver Physiol*. 2012;302:G1359–G1363.
45. Xu P, Becker H, Elizalde M, et al. Intestinal organoid culture model is a valuable system to study epithelial barrier function in IBD. *Gut*. 2018;67:1905–1906.
46. Van Itallie CM, Anderson JM. Claudins and epithelial paracellular transport. *Annu Rev Physiol*. 2006;68:403–429.
47. Mehta S, Nijhuis A, Kumagai T, et al. Defects in the adherens junction complex (E-cadherin/β-catenin) in inflammatory bowel disease. *Cell Tissue Res*. 2015;360:749–760.
48. Spence JR, Mayhew CN, Rankin SA, et al. Directed differentiation of human pluripotent stem cells into intestinal tissue in vitro. *Nature*. 2011;470:105–109.
49. Foulke-Abel J, In J, Kovbasnjuk O, et al. Human enteroids as an ex-vivo model of host-pathogen interactions in the gastrointestinal tract. *Exp Biol Med (Maywood)*. 2014;239:1124–1134.
50. Zachos NC, Kovbasnjuk O, Foulke-Abel J, et al. Human enteroids/colonoids and intestinal organoids functionally recapitulate normal intestinal physiology and pathophysiology. *J Biol Chem*. 2016;291:3759–3766.
51. Yu H, Hasan NM, In JG, et al. The contributions of human mini-intestines to the study of intestinal physiology and pathophysiology. *Annu Rev Physiol*. 2017;79:291–312.
52. Turner JR. Intestinal mucosal barrier function in health and disease. *Nat Rev Immunol*. 2009;9:799–809.
53. Rosenthal R, Milatz S, Krug SM, et al. Claudin-2, a component of the tight junction, forms a paracellular water channel. *J Cell Sci*. 2010;123:1913–1921.
54. Van Itallie CM, Holmes J, Bridges A, et al. The density of small tight junction pores varies among cell types and is increased by expression of claudin-2. *J Cell Sci*. 2008;121:298–305.
55. Van Itallie CM, Holmes J, Bridges A, et al. Claudin-2-dependent changes in noncharged solute flux are mediated by the extracellular domains and require attachment to the PDZ-scaffold. *Ann N Y Acad Sci*. 2009;1165:82–87.
56. Smyth D, Phan V, Wang A, et al. Interferon-γ-induced increases in intestinal epithelial macromolecular permeability requires the Src kinase Fyn. *Lab Invest*. 2011;91:764–777.
57. Rosen MJ, Frey MR, Washington MK, et al. STAT6 activation in ulcerative colitis: a new target for prevention of IL-13-induced colon epithelial cell dysfunction. *Inflamm Bowel Dis*. 2011;17:2224–2234.
58. Rosen MJ, Chaturvedi R, Washington MK, et al. STAT6 deficiency ameliorates severity of oxazolone colitis by decreasing expression of claudin-2 and Th2-inducing cytokines. *J Immunol*. 2013;190:1849–1858.
59. McKay DM, Botelho F, Ceponis PJ, et al. Superantigen immune stimulation activates epithelial STAT-1 and PI 3-K: PI 3-K regulation of permeability. *Am J Physiol Gastrointest Liver Physiol*. 2000;279:G1094–G1103.
60. Watson JL, Ansari S, Cameron H, et al. Green tea polyphenol (–)-epigallocatechin gallate blocks epithelial barrier dysfunction provoked by IFN-gamma but not by IL-4. *Am J Physiol Gastrointest Liver Physiol*. 2004;287:G954–G961.
61. McKay DM, Watson JL, Wang A, et al. Phosphatidylinositol 3'-kinase is a critical mediator of interferon-gamma-induced increases in enteric epithelial permeability. *J Pharmacol Exp Ther*. 2007;320:1013–1022.
62. Scharl M, Paul G, Weber A, et al. Protection of epithelial barrier function by the Crohn's disease associated gene protein tyrosine phosphatase n2. *Gastroenterology*. 2009;137:2030–2040.e5.
63. Yoshida H, Kimura A, Fukaya T, et al. Low dose CP-690,550 (tofacitinib), a pan-JAK inhibitor, accelerates the onset of experimental autoimmune encephalomyelitis by potentiating Th17 differentiation. *Biochem Biophys Res Commun*. 2012;418:234–240.
64. Rosengren S, Corr M, Firestein GS, et al. The JAK inhibitor CP-690,550 (tofacitinib) inhibits TNF-induced chemokine expression in fibroblast-like synoviocytes: autocrine role of type I interferon. *Ann Rheum Dis*. 2012;71:440–447.
65. Sandborn WJ, Ghosh S, Panes J, et al.; Study A3921063 Investigators. Tofacitinib, an oral Janus kinase inhibitor, in active ulcerative colitis. *N Engl J Med*. 2012;367:616–624.